J Neuropathol Exp Neurol
Vol. 73, No. 7
July 2014
pp. 684–692

ORIGINAL ARTICLE

OPEN

Involvement of Matrix Metalloproteinase-9 in Amyloid-β 1–42–Induced Shedding of the Pericyte Proteoglycan NG2

Nina Schultz, BS, Henrietta M. Nielsen, PhD, Lennart Minthon, MD, PhD, and Malin Wennström, PhD

Abstract

Deposition of amyloid-β (Aβ) 1–42, the major component of senile plaques characteristic of Alzheimer disease, affects brain microvascular integrity and causes blood-brain barrier dysfunction, increased angiogenesis, and pericyte degeneration. To understand the cellular events underlying Aβ1–42 effects on microvascular alterations, we investigated whether different aggregation forms of Aβ1–42 affect shedding of the pericyte proteoglycan NG2 and whether they affect proteolytic cleavage mediated by matrix metalloproteinase (MMP)-9. We found decreased levels of soluble NG2, total MMP-9, and MMP-9 activity in pericyte culture supernatants in response to fibril-enriched preparations of Aβ1–42. Conversely, oligomer-enriched preparations of Aβ1–42 increased soluble NG2 levels in the supernatants. This increase was ablated by the MMP-9/MMP-2 inhibitor SB-3CT. There was also a trend toward increased MMP-9 activity observed after oligomeric Aβ1–42 exposure. Our results, demonstrating an Aβ1–42 aggregation-dependent effect on levels of NG2 and MMP-9, support previous studies showing an impact of Aβ1–42 on vascular integrity and thereby add to our understanding of mechanisms behind the microvascular changes commonly found in patients with Alzheimer disease.

Key Words: Alzheimer disease, Amyloid-β, Matrix metalloproteinase-9, NG2 proteoglycan, Pericytes.

INTRODUCTION

Pericytes play a vital role in brain blood vessel function and integrity. Wrapped around the wall of capillaries, they stabilize the blood vessels and regulate blood flow by responding to vasoactive substances (1). Pericytes are also, as one of the key players in the neurovascular unit, important for the maintenance of the blood brain barrier (BBB) (2, 3), which protects the brain from periphery-derived harmful substances and controls influx of nutrients. This cell-type further expresses several BBB-related transporters, which implicates these cells in brain-to-blood efflux (4, 5). Since pericytes also have phagocytic properties (6), they are regarded as important actors in the clearance of neurotoxic substances from the brain parenchyma. In addition, pericytes regulate the formation of new blood vessels as they secrete angiogenic factors, for example, vascular endothelial growth factor (7) and matrix metalloproteinases (MMPs) (8, 9); MMPs proteolytically degrade the extracellular matrix, paving the way for migrating cells and sprouting blood vessels (10).

Recent studies have implicated pericytes in the pathogenesis of Alzheimer disease (AD) (11–13), which is foremost associated with a progressive accumulation of aggregated amyloid-β (Aβ) 1–42 and intraneuronal neurofibrillary tangles of hyperphosphorylated tau (14). The brains of AD patients also exhibit neuroinflammation (15), white matter changes (16, 17), and microvascular pathology. Microvascular abnormalities include BBB dysfunction, aberrant angiogenesis, altered microvascular density, and atrophic and ruptured microvessels (12, 13, 18–21)—events that may involve pericyte malfunction. Indeed, a recent study demonstrated an approximately 60% reduction of pericytes and blood vessel coverage in AD patients versus neurologically intact controls. The reduction in pericytes was shown to correlate with BBB dysfunction and amyloid plaque load (22). The involvement of pericytes in AD-associated pathology has been demonstrated as pericyte loss in transgenic mice overexpressing the Aβ precursor protein (APP); the mice also have elevated, impaired and accelerated Aβ clearance (11). Moreover, cultured human pericytes have decreased viability after prolonged exposure to the Aβ peptide (23, 24). Thus, changes in the pericyte population, possibly caused by the increasing load of toxic Aβ, may underlie some of the microvascular events and the impaired clearance of Aβ with accelerating neurodegenerative processes as downstream events (1).

Pericytes are recognized by their expression of the transmembrane proteoglycan NG2 (25, 26). This proteoglycan plays an important role in the interaction between endothelial cells and pericytes. Specific targeting of NG2

From the Clinical Memory Research Unit, The Wallenberg Laboratory, Department of Clinical Sciences Malmö, Lund University, Malmö, Sweden (NS, LM, MW); and Department of Neuroscience, Mayo Clinic, Jacksonville, Florida (HMN).

Send correspondence and reprint requests to: Malin Wennström, PhD, Clinical Memory Research Unit, The Wallenberg Laboratory, Department of Clinical Sciences Malmö, Lund University, Skåne University Hospital, Second Floor, Inga Marie Nilssons gata, Entrance 53, Malmö 205 02, Sweden; E-mail: malin.wennstrom@med.lu.se

This work was supported by The Swedish Dementia Foundation (Malin Wennström), ALF (Henrietta M. Nielsen, Lennart Minthon, Malin Wennström), Swedish brainpower (Lennart Minthon), Söderström Königska Foundation (Malin Wennström), Sigurd and Elsa Goljes Memory Foundation (Malin Wennström), and Kocks Stiftelser (Malin Wennström).

Malin Wennström had full access to all data in the study and takes responsibility for the integrity of the data and the accuracy of data analysis.

Supplemental digital content is available for this article. Direct URL citations appear in the printed text and are provided in the HTML and PDF versions of this article on the journal's Web site (www.jneuropath.com).

using anti-NG2 antibodies inhibits ischemia-induced retinal angiogenesis in mice (27). Decreased pericyte ensheathment of endothelial cells, diminished formation of endothelial cells, and reduced assembly of the vascular basal lamina have been demonstrated in pericyte-specific NG2-null mice (28). In vitro studies have also demonstrated that NG2 knockdown in pericytes inhibits 3-dimensional pericyte–endothelial cell network formation, pericyte proliferation/migration, and endothelial cell junction formation, which leads to increased endothelial cell monolayer permeability (28). Interestingly, shed soluble NG2 (sNG2) has been shown to promote angiogenesis and migration of endothelial cells via binding of sNG2 to ligands expressed on endothelial cells (29).

We have previously demonstrated decreased levels of sNG2 and a correlation between sNG2 and Aβ1–42 in the cerebrospinal fluid (CSF) of patients with AD (30). We have also shown decreased CSF sNG2 levels in patients with dementia with Lewy bodies, but not in patients with Parkinson disease (31). Both of these disorders are neuropathologically characterized by abnormal intraneuronal inclusions of alpha (α)-synuclein (Lewy bodies), but DLB patients may also display Aβ plaques similar to AD patients (32). We further demonstrated a direct inhibiting effect of fibrillar Aβ1-42 on NG2 shedding from cultured primary human oligodendrocyte precursor cells (OPC) (30), which also express NG2 (33). The mechanisms behind Aβ-induced NG2 shedding are not known, but MMPs, in particular MMP-9, have been shown to affect NG2 shedding in general. Broad-spectrum MMP inhibitors have been reported to decrease the amount of sNG2 in conditioned media from cultured rat oligodendrocyte precursor cells (34), and decreased sNG2 levels in rat spinal cord after infusion of the MMP-9/MMP-2 inhibitor SB-3CT have also been demonstrated (35). It has further been shown that NG2 is a substrate for MMP-9 (36) and that clearance of NG2 from injured brain areas is lost in MMP-9–null mice (36).

Whether Aβ1–42 also affects pericyte NG2 shedding and whether MMP-9 is the sheddase involved are not known. Here, we analyzed sNG2 levels in primary human pericyte culture supernatants after exposure to fibril- and oligomer-enriched Aβ1–42 preparations in the presence or in the absence of the MMP-9/MMP-2 inhibitor SB-3CT. We next measured the activities of MMP-9 and MMP-2 after exposure to fibrillar and oligomeric Aβ1–42. Lastly, we analyzed the impact of Aβ1–42 on cell viability and total concentrations of MMP-9, MMP-1, and MMP-3; the two latter MPPs are known to affect MMP-9 production and activity (37–39).

MATERIALS AND METHODS

Cells

Primary human brain vascular pericytes (HBVPs) isolated from fetal brain tissue (ScienCell Research Laboratories, San Diego, CA) were cultured in pericyte culture media (ScienCell Research Laboratories) containing 2% fetal bovine serum. Cells were grown as monolayers in poly-L-lysine–coated culture flasks in humidified air with 5% CO_2 at 37°C until they were 80% to 90% confluent. Before the experiments, the cells were plated onto either 12-well chamber slides (Nunc A/S) or 8-well chamber slides (Lab-Tek) and grown until 80% confluent. Cell population purity was assessed by immunofluorescence staining using antibodies against NG2 (1:200; Millipore, Billerica, MA), platelet-derived growth factor receptor-β (PDGFR-β) (1:200; Abcam, Cambridge, MA), and α-smooth muscle actin (αSMA) (Sigma, St Louis, MO). Cells were fixed in 2% formaldehyde, incubated with blocking solution (PBS containing 1% BSA [Boehringer Mannheim, Vienna, Austria] and 5% goat serum [Jackson ImmunoResearch, West Grove, PA]) and thereafter incubated with the primary antibodies (anti-NG2 and anti-PDGFR-β in blocking solution) followed by an incubation with the appropriate secondary antibodies Alexa 488-conjugated anti-rabbit immunoglobulin G (IgG) (1:500 Molecular Probes) or Cy3-conjugated antimouse IgG (1:500, Jackson ImmunoResearch). Cells stained against SMA were fixed in 2% formaldehyde, permeabilized with 0.1% Saponin (Sigma-Aldrich) in 1% bovine serum albumin (BSA)/PBS, incubated with blocking solution, and incubated with Cy3-conjugated antibodies directed against anti-αSMA (1:200, Sigma). Finally, cells were mounted with Vectashield Set mounting medium with DAPI (Vector Laboratories, Burlingame, CA). The morphology of the cells corresponded well to previously published images of HBVP (40, 41); the percentage of DAPI-positive/NG2-positive/PDGFR-β–positive cells of total DAPI-positive cells (n = 250) was approximately 99% (Fig. 1). In line with previous studies on primary pericytes isolated from human and rodent brain tissues (42, 43), few (<1%) of the

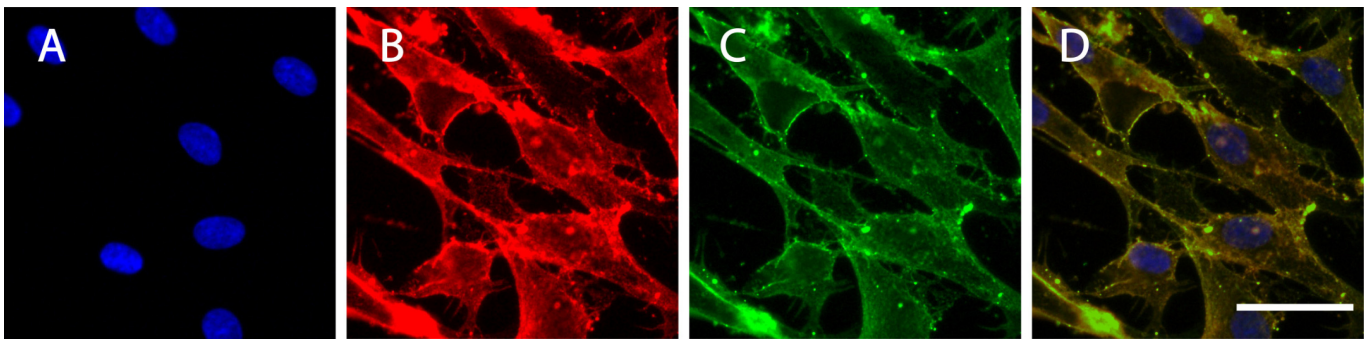

FIGURE 1. Fetal HBVPs express the pericyte protein NG2 and PDGFR-β. Human brain vascular pericyte stained with DAPI **(A)**, anti-NG2 antibody **(B)**, and anti–PDGFR-β antibody **(C)**. Images are merged in **(D)**. Scale bar = 10 μm.

HBVPs expressed αSMA, indicating an undifferentiated state of the HBVPs.

Aβ Preparations

Aβ1–42 oligomer- and fibril-enriched preparations were prepared by dissolving Aβ1–42 peptide (Bachem, Bubendorf, Switzerland) in cold hexaflouro-2-propanol (Sigma-Aldrich/Fluka), aliquoted, dried by speed vacuum, and stored at −80°C until used. Before cell treatment, hexaflouro-2-propanol/Aβ1–42 was dissolved in dimethyl sulfoxide (DMSO) to a final concentration of 2.5 mmol/L and sonicated for 10 minutes. For oligomeric preparation, Aβ1–42/DMSO was diluted to 100 μmol/L in phenol red–free Dulbecco modified Eagle medium and incubated for 24 hours at 4°C. Fibrillar preparations were generated by diluting Aβ1–42/DMSO to 100 μmol/L in 10 mmol/L HCl then incubated for 24 hours at 37°C. Differences between fibril-enriched and oligomer-enriched Aβ1–42 preparations before and after treatment of HBVPs were documented by Western blot analysis (Figure, Supplemental Digital Content 1, http://links.lww.com/NEN/A602). The Aβ1–42 preparations were separated on 10% Tris-tricine gels and transferred to polyvinylidene difluoride membranes (Millipore) using a transblot semidry transfer cell (BioRad, Hercules, CA) at room temperature for 60 minutes at a current of 50 mA. The membranes were rinsed, incubated with blocking solution (PBS-Tween containing 5% milk powder; Fluka) for 1 hour, and incubated with mouse anti–Aβ1–16 6E10 antibody (1:5000; Covance, Princeton, NJ) in blocking solution on a shaker at 4°C. The membranes were rinsed and incubated with anti-mouse Na931V antibody (1:1000; GE Healthcare, Deigen, Belgium) for 1 hour at room temperature on a shaker. Proteins were visualized using the Luminata Forte Western HRP Substrate (Millipore) and a LAS-3000 charge-coupled device camera (FujiFilm).

HBVP Treatment

Before cell treatment, the pericyte culture media were removed and replaced with serum-free culture media (ScienCell Research Laboratories) containing 10 μmol/L Aβ1–42 fibril-enriched preparations and 10 μmol/L Aβ1–42 oligomer-enriched preparations. Cells were treated with DMSO/phenol red–free Dulbecco modified Eagle medium (vehicle for Aβ1–42 oligomer-enriched preparations) and DMSO/HCl (vehicle for Aβ1–42 fibril-enriched preparations) as controls. Potential involvement of MMP-9 in Aβ1–42–regulated NG2 shedding was analyzed by adding 10 μmol/L of the MMP-9/MMP-2 inhibitor SB-3CT (Calbiochem, Billerica, MA) to HBVPs exposed to vehicles, 10 μmol/L Aβ1–42 fibril-enriched preparations, or 10 μmol/L Aβ1–42 oligomer-enriched preparations. The cells were incubated for 24 hours at 37°C. All experiments were performed in duplicate and repeated independently 3 times. Cell culture supernatants were collected after treatment, centrifuged (275 × *g*, 5 minutes, 4°C), aliquoted, and stored at −80°C until used. The cells were rinsed with PBS, lysed with the mammalian Cell Lysis Kit (Sigma-Aldrich) according to the manufacturer's protocol, aliquoted, and stored at −80°C until used. Similar protein concentrations in the wells with different treatment conditions were verified with the Bradford (Coomassie plus) assay kit (Thermo Scientific).

NG2 Quantification Assay

Levels of NG2 in HBVP cell culture supernatants and lysates were analyzed on an in-house–developed assay with Meso Scale Discovery electrochemiluminescence technology using immunoassay conversion kits (Meso Scale Discovery, Rockville, MD). Cell culture supernatants and lysates were diluted (1:5 and 1:250, respectively) in PBS and coated onto Meso Scale Discovery high-bind plates in triplicate wells (25 μL) and allowed to adhere overnight at 4°C with slow agitation. The wells were thereafter washed with washing buffer (0.05% Tween 20 in PBS) and incubated with blocking solution (1% bovine serum albumin and 1% milk in PBS-Tween) for 1 hour. After rinse, the wells were incubated with mouse anti-NG2 (1:100, ATCC clone B5; kind gift from Dr William Stallcup, Burnham Institute, La Jolla, CA) for 2 hours on a shaker, washed, and incubated with goat anti-mouse sulftag-conjugated secondary antibodies (1:500; Meso Scale Discovery) for 1 hour on a shaker. The electrochemiluminescence signal was quantified using a Meso Scale Discovery SECTOR Imager 6000.

MMP-9 and MMP-2 Activity Assays

SensoLyte Plus 520 MMP-9 and MMP-2 Assay Kits (AnaSpec, Fremont, CA) were used according to the manufacturer's instructions to quantify MMP-9 and MMP-2 activities in HBVP cell culture supernatants. The assays are MMP-9– and MMP-2–specific, with no cross-reactivity with other MMPs. The MMP activity unit was expressed as the change in fluorescence intensity (relative fluorescence unit) at an excitation of 490 nm and at an emission of 520 nm. The emission at 520 nm was measured after 1 hour using the Microplate Spectophotometer Infinite M200 and the Magellan version 3.5 software.

MMP Quantification

Human MMP 3-Plex Ultra-Sensitive immunoassay (Meso Scale Discovery, Oxford, United Kingdom) was used according to the manufacturer's protocol to quantify both the active and the proenzyme forms of MMP-1, MMP-3, and MMP-9. Detection limits for MMP-1, MMP-3, and MMP-9 in HBVP cell culture supernatants were 3.15, 3.39, and 11.8 pg/mL, respectively.

Lactic Dehydrogenase Cytotoxicity Assay

Cell viability was determined as a measure of lactic dehydrogenase (LDH) activity in HBVP cell culture supernatants, as previously described (30, 44). Supernatants from control cell cultures treated with vehicle for Aβ1–42 fibril-enriched or oligomer-enriched preparations were used as baseline controls; supernatants from cells treated with 1 μmol/L staurosporine (Sigma-Aldrich) for 24 hours were used as positive controls for cytotoxicity. *K* values obtained were averaged (mean ± SD) and expressed as percentage of activity in cell culture supernatants from baseline controls.

Statistical Analysis

Statistical analysis was performed using the SPSS software (version 20 for Windows; SPSS Inc, Chicago, IL). To detect significant differences between the different experimental conditions, we analyzed the data using paired t-test.

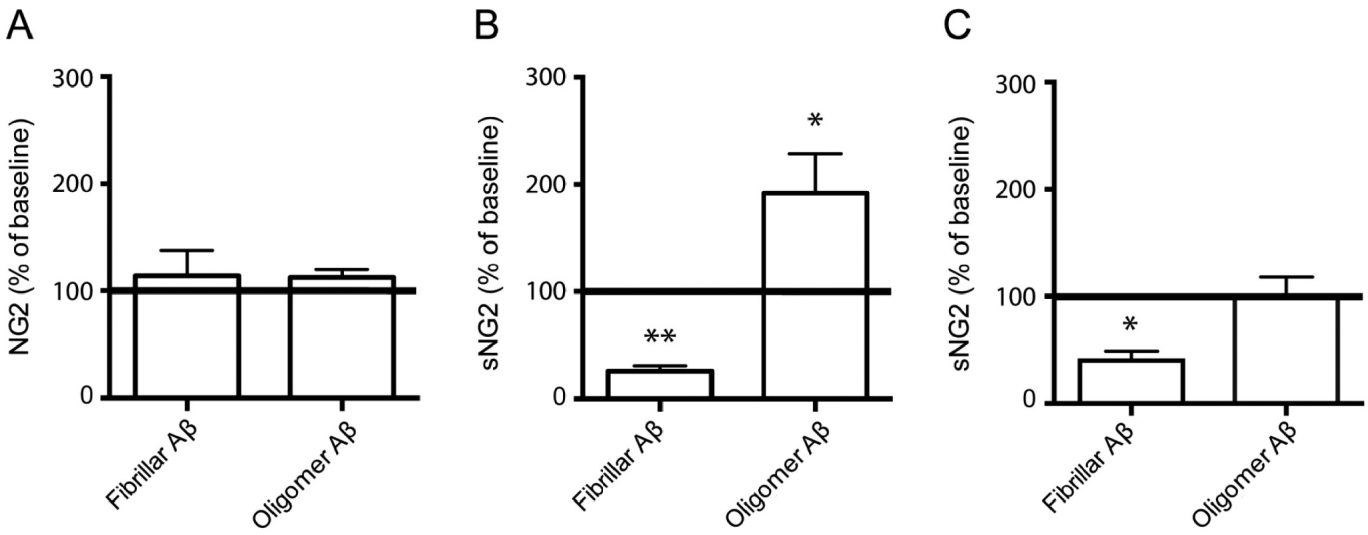

FIGURE 2. Bar graphs demonstrating alterations in the levels of the pericyte protein NG2 in cell culture supernatants and lysates from HBVPs after exposure to 10 μmol/L oligomer- or fibril-enriched Aβ 1–42 preparations for 24 hours in the presence or in the absence of the MMP-9/MMP-2 inhibitor SB-3CT. **(A)** No alterations in NG2 levels were found in HBVP lysates after exposure to either fibril- or oligomer-enriched Aβ1–42 preparations. **(B)** Exposure to fibrillar Aβ1–42 significantly decreased, whereas oligomeric Aβ1–42 significantly increased, the levels of sNG2 (% of vehicle). **(C)** The increased levels of sNG2 in HBVP cell culture supernatants observed after exposure to oligomer-enriched Aβ1–42 preparations were inhibited in the presence of SB-3CT. Data were analyzed using paired t-test. * Significant difference at $p < 0.05$ level versus baseline. ** Significant difference at $p < 0.01$ level versus baseline.

Results are presented as mean ± SD. A value of $p < 0.05$ was considered significant.

RESULTS

Aβ1–42 Alters sNG2 Levels in an Aggregation-Dependent Manner

Initially, we investigated whether fibril- and oligomer-enriched preparations of Aβ1–42 differently affect HBVP levels of surface-bound or shed NG2. Analysis of HBVP lysates demonstrated unaltered NG2 levels after exposure to both oligomeric and fibrillar Aβ1–42 versus vehicle (Fig. 2A; Table). Levels of sNG2 in HBVP culture supernatants were, however, significantly decreased compared with vehicle control upon exposure to fibrillar Aβ1–42 (Fig. 2B; Table). In contrast, sNG2 levels were significantly increased compared with vehicle upon oligomeric Aβ1–42 exposure ($p = 0.036$) (Fig. 2B; Table).

SB-3CT Ablates Oligomeric Aβ1–42–Induced NG2 Shedding

Previous studies have shown decreased levels of sNG2 in rat spinal cord after infusion of the MMP-9/MMP-2 inhibitor SB-3CT. Therefore, we investigated whether SB-3CT affects Aβ-induced NG2 shedding. In the presence of SB-3CT, the levels of sNG2 from HBVPs exposed to fibrillar Aβ1–42 remained significantly decreased versus

TABLE. Variables Analyzed in HBVP Lysate and Cell Culture Supernatants After Aβ1–42 Exposure

	Treatment			
Variables	**Vehicle Fibrillar Aβ1–42**	**Fibrillar Aβ1–42**	**Vehicle Oligomeric Aβ1–42**	**Oligomeric Aβ1–42**
NG2 lysate, μg/mL	94.76 ± 33.05	104.90 ± 39.71	98.59 ± 0.25	112.09 ± 0.35
sNG2 cell sup, μg/mL	1.23 ± 0.49	0.29 ± 0.13*	0.98 ± 0.34	1.74 ± 0.52†
+ SB-3CT sNG2 cell sup, μg/mL	1.20 ± 0.40	0.47 ± 0.16‡	1.27 ± 0.45	1.24 ± 0.34
Total MMP-9 cell sup, pg/mL	138.83 ± 13.08	74.41 ± 28.89†	136.54 ± 15.21	113.13 ± 13.41
Total MMP-1 cell sup, ng/mL	16.98 ± 3.88	5.19 ± 2.13*	17.99 ± 3.78	14.04 ± 3.44
Total MMP-3 cell sup, pg/mL	21.61 ± 3.46	10.65 ± 4.55	27.62 ± 13.27	13.26 ± 3.55*
MMP-9 activity cell sup, RFU	3359 ± 552	1515 ± 688*	1802 ± 1167	2736 ± 342
MMP-2 activity cell sup, RFU	3874 ± 2187	4006 ± 2298	2391 ± 1228	2366 ± 1266

Data were analyzed using paired t-test and are presented as mean ± SD.
* $p < 0.01$ level versus vehicle.
† $p < 0.05$ level versus vehicle.
‡ $p < 0.001$ level versus vehicle.
Cell sup, cell culture supernatant; RFU, relative fluorescence units.

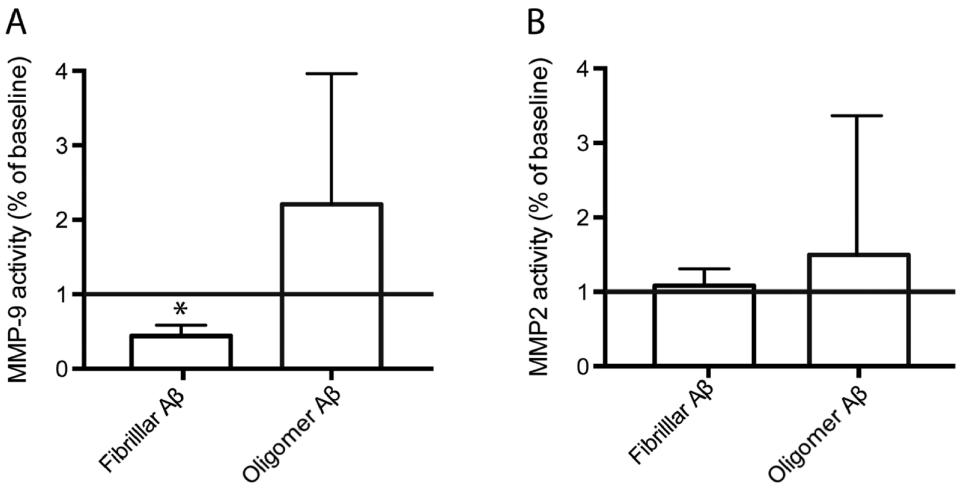

FIGURE 3. Bar graphs demonstrating alterations in total MMP-9 and MMP-2 activities in cell culture supernatants from HBVPs after exposure to 10 μmol/L oligomer- or fibril-enriched Aβ 1–42 preparations for 24 hours. **(A)** Exposure to fibrillar Aβ1–42 significantly decreased MMP-9 activity (% of vehicle), whereas no significant change was found after oligomeric Aβ1–42 exposure. **(B)** No alterations in MMP-2 activity were found in HBVP cell culture supernatants after exposure to either fibrillar or oligomeric Aβ1–42. Data were analyzed with paired t-test. * Significant difference at $p < 0.05$ level versus baseline.

those for vehicle (Fig. 2C; Table). The described increase in sNG2 levels after exposure to oligomeric Aβ1–42 was ablated in the presence of SB-3CT (Fig. 2C; Table).

Aβ1–42 Alters the Activity of MMP-9, But Not MMP-2, in an Aggregation-Dependent Manner

We next analyzed the activities of MMP-9 and MMP-2 when inhibited by SB-3CT in HBVP culture supernatants after exposure to oligomeric and fibrillar Aβ1–42. There was a significant decrease in MMP-9 activity after exposure to fibrillar Aβ1–42 versus vehicle (Fig. 3A; Table). On the contrary, oligomeric Aβ1–42 increased MMP-9 activity; however, although the results from all 3 independent experiments consistently showed higher MMP-9 activity in oligomeric Aβ1–42–exposed HBVPs compared with the respective vehicle, this increase did not reach significance (Fig. 3A; Table). Activity of MMP-2 did not change after exposure to either oligomeric or fibrillar Aβ1–42 compared with vehicle (Fig. 3B; Table).

Aβ1–42 Alters MMP-9 and MMP-1 Levels in an Aggregation-Dependent Manner

Because our results support the notion of MMP-9 as a candidate sheddase involved in Aβ1–42–altered NG2 shedding, we measured total protein levels (active enzyme and proenzyme) of MMP-9 in Aβ1–42–exposed HBVP culture

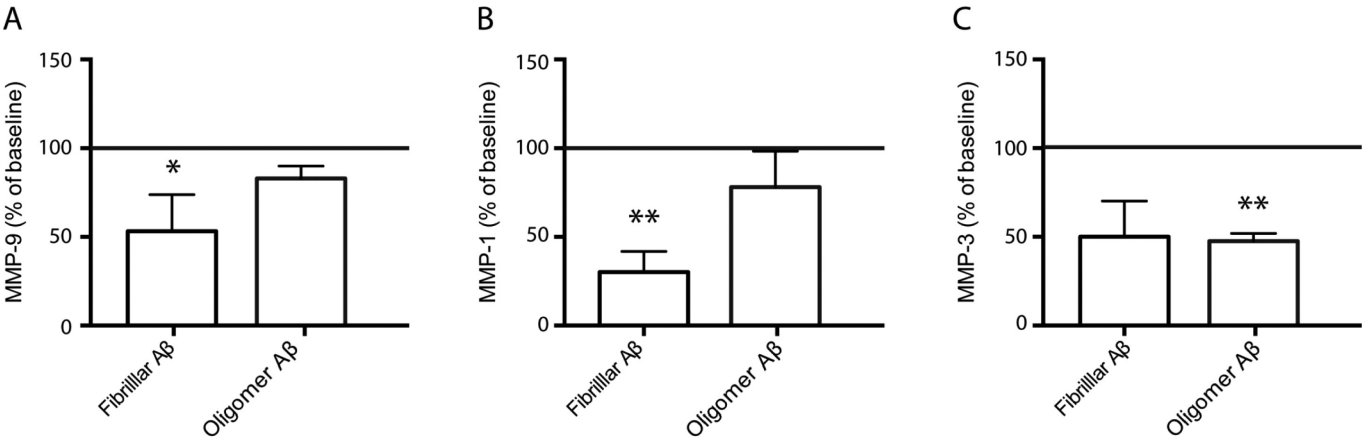

FIGURE 4. Bar graphs demonstrating alterations in total MMP-9, MMP-1, and MMP-3 levels in cell culture supernatants from HBVPs after exposure to 10 μmol/L oligomer- or fibril-enriched Aβ 1–42 preparations for 24 hours. **(A)** Exposure to fibrillar Aβ1–42 significantly decreased total MMP-9 levels (% of vehicle), whereas no change in MMP-9 levels was found after oligomeric Aβ1–42 exposure. **(B)** Levels of total MMP-1 (% of vehicle) were significantly reduced after fibrillar Aβ1–42 exposure but were unaltered after oligomeric Aβ1–42 exposure. **(C)** There was a significant reduction in total MMP-3 levels (% of vehicle) after oligomeric Aβ1–42 exposure, but significance was not reached after fibrillar Aβ1–42 exposure. Data were analyzed with paired t-test. * Significant difference at $p < 0.05$ level versus baseline. ** Significant difference at $p < 0.01$ level versus baseline.

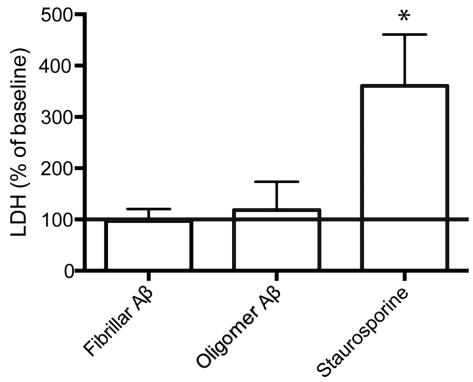

FIGURE 5. Bar graphs demonstrating alterations in LDH activity, indicative of cell viability, in cell culture supernatants from HBVPs after exposure to 10 μmol/L oligomer- or fibril-enriched Aβ1–42 preparations for staurosporine for 24 hours. Viability of HBVP was not altered after exposure to oligomeric or fibrillar Aβ1–42 but was significantly increased in response to the positive control staurosporine. Data were analyzed with paired t-test. * Significant difference at $p < 0.05$ level versus baseline.

supernatants. Although MMP-9 concentrations remained unaltered upon treatment with oligomeric Aβ1–42, there were significantly decreased MMP-9 concentrations after fibrillar Aβ1–42 exposure (Fig. 4A; Table). We also measured total levels of MMP-3 and MMP-1—MMPs known to affect MMP-9 activity and production (37–39). Total MMP-1 concentrations were, like those of MMP-9, significantly reduced in the presence of fibrillar Aβ1–42, but not oligomeric Aβ1–42, compared with vehicle (Fig. 4B; Table). By contrast, significantly reduced levels of MMP-3 were found after oligomeric Aβ1–42, but not fibrillar Aβ1–42, exposure (Fig. 4C; Table).

Aβ1–42 Exposure Does Not Alter Pericyte Viability

To rule out the possibility that the observed alterations in sNG2 levels resulted from Aβ1–42– induced cell death, we measured extracellular LDH activity (as an indication of cell death) in culture supernatants from HBVPs exposed to oligomeric and fibrillar Aβ1–42. As expected, cells exposed to the positive control staurosporine demonstrated significantly increased extracellular LDH activity versus vehicle-treated cells, but no alterations in LDH activity were found after exposure to either fibrillar or oligomeric Aβ1–42 (Fig. 5).

DISCUSSION

We recently demonstrated decreased levels of sNG2 in the CSF of patients with AD (30) and dementia with Lewy bodies (31), both of which are associated with extracellular deposition of Aβ. Our previous results also demonstrated decreased NG2 immunoreactivity in the vicinity of amyloid plaques in individuals with significant plaque loads. We further showed that the levels of sNG2 are decreased in culture supernatants from NG2-expressing HOPCs exposed to fibrillar Aβ1–42 (30). Extending our previous findings, we show here that the Aβ-induced decrease in NG2 is not cell-specific because fibrillar Aβ1–42 also significantly decreased sNG2 levels in the culture supernatant from primary human pericytes. We also show that in contrast to fibrillar Aβ1-42, oligomeric Aβ1-42 significantly increased sNG2 levels in cultured pericytes, whereas the contents of the HBVP lysate NG2 remained unaltered. Together, these results demonstrate an aggregation-dependent effect of Aβ1–42 on NG2 shedding from the cell surface.

Interestingly, the oligomeric Aβ1–42–induced increase in sNG2 was ablated in the presence of SB-3CT. Activity of MMP-9 was significantly lower after fibrillar Aβ1–42 exposure, whereas a slight increase in activity after oligomeric Aβ1–42 exposure did not reach significance. No alteration in MMP-2 activity was detected after exposure to either Aβ1–42 aggregation form. Fibrillar Aβ1–42 furthermore decreased the total levels of MMP-9 and MMP-1, but not MMP-3, whereas oligomeric Aβ1–42 did not affect the levels of MMP-9 or MMP-1 but significantly decreased the level of MMP-3. Finally, neither Aβ1–42 aggregation form affected HBVP viability.

In our previous study on HOPCs, we did not detect any difference in sNG2 levels after oligomeric Aβ1–42 exposure (30). Thus, as previously suggested by Asher et al (34), the presence of active NG2 sheddase is cell type–dependent (i.e. the enzyme responsible for Aβ1–42–induced enhanced proteolytic cleavage of NG2 in HBVP cultures may not be secreted or is inhibited in HOPC cultures). This hypothesis is strengthened by the fact that Asher et al (34) did not find an inhibitory effect on rat oligodendrocyte precursor cell NG2 shedding in the presence of metallopeptidase inhibitor-1 (TIMP-1), an inhibitor that acts on MMPs, including MMP-9. In the present study, we demonstrated an inhibitory effect of the MMP-9/MMP-2 inhibitor SB-3CT on oligomeric Aβ-induced NG2 shedding.

To determine whether the effect of SB-3CT was caused by an inhibitory effect on MMP-9 or MMP-2 activity, we measured the activities of both MMPs after Aβ1–42 exposure. In agreement with the altered sNG2 levels, we found decreased MMP-9 activity after fibrillar Aβ1–42 exposure and a trend toward increased MMP-9 activity after oligomeric Aβ1–42 exposure. By contrast, MMP-2 activity was unaltered after exposure to either aggregation variant. These results support the idea that an Aβ1–42–induced alteration in NG2 shedding is mediated specifically via the MMP-9 pathway and not via the MMP-2 pathway.

Our analysis of total MMP levels (i.e. proenzymes, active enzymes, and enzyme/inhibitor complexes) again showed a decrease in MMP-9 after fibrillar Aβ1–42 exposure, indicating a decrease in MMP-9 secretion in response to this Aβ1–42 aggregation form. Surprisingly, although oligomeric Aβ1–42 stimulation increased MMP-9 activity, it did not increase total MMP-9 levels. This incongruence suggests that secretion of MMP-9 is not altered in response to oligomeric Aβ1–42; rather, there is a shift in the proenzyme/active enzyme ratio or a shift in activated enzyme/inhibited enzyme that underlies the unaltered total MMP-9 level. This result further underscores the importance of carefully differentiating the interpretation of different MMP-9 assays.

Our total MMP analysis also demonstrated an aggregation-dependent impact of Aβ1–42 on total levels of MMP-1 and

MMP-3. Both MMPs have been shown to enhance MMP-9 expression in macrophages (39), and MMP-3 is known to activate the proenzyme MMP-9 (37, 38, 45). Our study instead showed that secretion of MMP-3 in response to the 2 Aβ1–42 preparations was altered in the opposite direction compared with secretion of MMP-9 and MMP-1. Although this result is not in line with the previous study on macrophages, our study is in agreement with a clinical study demonstrating decreased levels of MMP-9 and increased levels of MMP-3 in plasma from patients with AD (46).

The aggregation-dependent impact of Aβ1–42 on NG2 shedding and MMP secretion is highly relevant in view of the increasing number of studies supporting the idea that soluble oligomeric—not fibrillar—Aβ1–42 is the causative agent in the pathogenesis of AD (47, 48). For example, studies on the Tg2576 AD mouse model have shown hypervascularization, tight junction disruption, and BBB dysfunction after an early rise in amyloid precursor protein expression even before the onset of cognitive deficits and the presence of senile plaques (49, 50). In addition, active Aβ immunization was shown to a reverse these microvascular pathologic events (51, 52). These findings propose an impact of Aβ on BBB integrity even at the early stages of AD pathology and, more importantly, suggest that the soluble oligomeric Aβ1–42 or other Aβ species (rather than the senile plaque-forming fibrillar Aβ1–42) may be the culprits in Aβ-mediated BBB dysfunction. Our study demonstrates a significant increase in NG2 shedding in response to high levels of oligomeric Aβ1–42, in line with the concept previously presented by Biron et al (49). Based on the notion that amyloidogenesis in part underlies the microvascular pathology observed at the early stages of AD, the previously reported involvement of NG2 in angiogenesis and BBB integrity, and our findings in the current study, it is tempting to hypothesize around the occurrence of the following scenario (Fig. 6): At the early stages of AD pathogenesis (i.e. before symptoms and cognitive decline become evident in patients with AD), pericytes respond to elevated levels of toxic oligomeric Aβ1–42 by secreting less MMP-9 inhibitors. Increased MMP-9 activity would lead to enhanced degradation of the extracellular matrix and tight junction proteins, thereby paving the way for cell migration across the BBB and along the vasculature (10, 53, 54). As a consequence, the MMP-9 substrate NG2 is shed from the cell surface of pericytes, thereby contributing to a loss of junctional interaction between pericytes and endothelial cells and between endothelial tight junctions (28, 55), leading to a dysfunctional BBB. The increased availability of sNG2 levels would also promote angiogenic activity (29) and, in combination with increased BBB permeability (56, 57) and degeneration of pericytes (23, 24, 58), blood vessels would be rendered unstable, disrupted, and leaky, which would eventually lead to microbleeds and incomplete infarcts (59, 60). As the pathology progresses, fibrillar Aβ1–42 accumulates and inhibits the cleavage of NG2 (30). This event could possibly be viewed as a protective mechanism, but the drastic loss (i.e. below normal levels) of available sNG2 may also reflect the loss of a factor involved in several crucial cellular events, including neuronal guidance, cell proliferation, and cell migration (26, 61). Support for the involvement of MMP-9 in the early pathogenesis of AD can be found in a previous clinical biomarker study demonstrating increased MMP-9 in the CSF of cognitively healthy elders with risk markers for future AD (62). Moreover, BBB dysfunction in mice carrying the APOEϵ4 genotype (a strong genetic risk factor for AD) was previously shown to be mediated by the proinflammatory cytokine cyclophilin A, which in turn promotes MMP-9 production. Remarkably, the BBB impairment in these mice could be reversed by SB-3CT treatment and specific inhibition of MMP-9, but not of MMP-2 (63). Whether CSF NG2 levels are altered at the early stages of AD pathogenesis remains to be investigated, but the previously reported decrease in CSF NG2 levels in AD patients (30) could possibly result from the inhibitory impact of fibrillar Aβ1–42 observed in our studies. Notably, the NG2 research field is still in its infancy, and we lack direct evidence for an impact of pericyte NG2 shedding on the vascular integrity of the BBB. We would, therefore, emphasize the importance of further investigations into the role of NG2 shedding in BBB integrity, preferably using experimental in vivo rodent models or clinical studies.

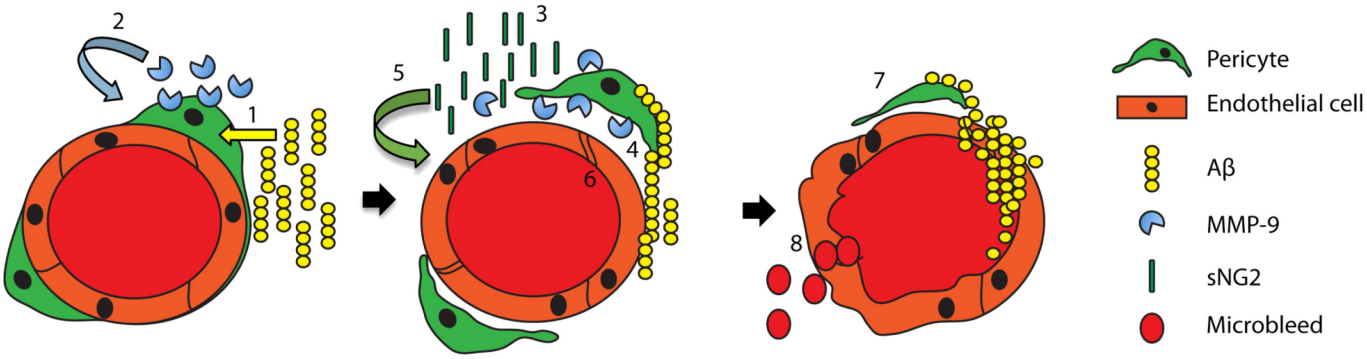

FIGURE 6. Image illustrating the hypothesized role of sNG2 in Aβ-induced microvascular pathology, as follows: 1) in response to increased levels of toxic oligomeric Aβ; 2) pericytes secrete extracellular MMPs, including MMP-9; 3) increased activated MMP-9 enhances NG2 shedding; 4) loss of extracellular matrix resulting from MMP-9 proteolysis causes pericytes to detach from the blood vessel; 5) the increased amount of sNG2 induces proliferation of endothelial cells; 6) BBB permeability increases; 7) extended exposure to Aβ degenerates pericytes; 8) lost pericyte support and fragility lead to rupture of microvessels.

In conclusion, the results from our study demonstrate an aggregation-dependent impact of Aβ1–42 on the shedding of pericyte NG2, a proteoglycan known to play a regulatory role in the maintenance of vascular integrity. Moreover, our study highlights MMP-9 as one of the mediators of Aβ1–42–induced alteration in NG2 shedding. These results are in line with the hypothesis suggesting amyloidogenesis as an event implicated in the microvascular pathology commonly found at the early stages of AD pathogenesis and highlight pericytes (possibly via the NG2 proteoglycan) as potential players in the events occurring in early AD pathogenesis.

ACKNOWLEDGMENTS

We thank Camilla Orbjörn for technical support and Dr William Stallcup (Burnham Institute) for the B5 antibody and the NG2 recombinant.

REFERENCES

1. Winkler EA, Bell RD, Zlokovic BV. Central nervous system pericytes in health and disease. Nat Neurosci 2011;14:1398–405
2. Armulik A, Genove G, Mae M, et al. Pericytes regulate the blood-brain barrier. Nature 2010;468:557–61
3. Bell RD, Winkler EA, Sagare AP, et al. Pericytes control key neurovascular functions and neuronal phenotype in the adult brain and during brain aging. Neuron 2010;68:409–27
4. Shimizu F, Sano Y, Maeda T, et al. Peripheral nerve pericytes originating from the blood-nerve barrier expresses tight junctional molecules and transporters as barrier-forming cells. J Cell Physiol 2008;217:388–99
5. Vagnucci AH Jr, Li WW. Alzheimer's disease and angiogenesis. Lancet 2003;361:605–8
6. Thomas WE. Brain macrophages: On the role of pericytes and perivascular cells. Brain Res Brain Res Rev 1999;31:42–57
7. Darland DC, Massingham LJ, Smith SR, et al. Pericyte production of cell-associated VEGF is differentiation-dependent and is associated with endothelial survival. Dev Biol 2003;264:275–88
8. Arihiro S, Ohtani H, Hiwatashi N, et al. Vascular smooth muscle cells and pericytes express MMP-1, MMP-9, TIMP-1 and type I procollagen in inflammatory bowel disease. Histopathology 2001;39:50–59
9. Takata F, Dohgu S, Matsumoto J, et al. Brain pericytes among cells constituting the blood-brain barrier are highly sensitive to tumor necrosis factor-alpha, releasing matrix metalloproteinase-9 and migrating in vitro. J Neuroinflamm 2011;8:106
10. Chen Q, Jin M, Yang F, et al. Matrix metalloproteinases: Inflammatory regulators of cell behaviors in vascular formation and remodeling. Mediators Inflamm 2013;2013:928315
11. Sagare AP, Bell RD, Zhao Z, et al. Pericyte loss influences Alzheimer-like neurodegeneration in mice. Nat Commun 2013;4:2932
12. Zlokovic BV. Neurovascular mechanisms of Alzheimer's neurodegeneration. Trends Neurosci 2005;28:202–8
13. Zlokovic BV. Neurovascular pathways to neurodegeneration in Alzheimer's disease and other disorders. Nat Rev Neurosci 2011;12:723–38
14. Blennow K, de Leon MJ, Zetterberg H. Alzheimer's disease. Lancet 2006;368:387–403
15. Lee YJ, Han SB, Nam SY, et al. Inflammation and Alzheimer's disease. Arch Pharm Res 2010;33:1539–56
16. Brun A, Englund E. A white matter disorder in dementia of the Alzheimer type: A pathoanatomical study. Ann Neurol 1986;19:253–62
17. Englund E, Brun A. White matter changes in dementia of Alzheimer's type: The difference in vulnerability between cell compartments. Histopathology 1990;16:433–39
18. Farkas E, Luiten PG. Cerebral microvascular pathology in aging and Alzheimer's disease. Prog Neurobiol 2001;64:575–611
19. Kalaria RN. Vascular basis for brain degeneration: Faltering controls and risk factors for dementia. Nutr Rev 2010;68(Suppl 2):S74–87
20. Marchesi VT. Alzheimer's dementia begins as a disease of small blood vessels, damaged by oxidative-induced inflammation and dysregulated amyloid metabolism: Implications for early detection and therapy. FASEB J 2011;25:5–13
21. Iadecola C. Neurovascular regulation in the normal brain and in Alzheimer's disease. Nat Rev Neurosci 2004;5:347–60
22. Sengillo JD, Winkler EA, Walker CT, et al. Deficiency in mural vascular cells coincides with blood-brain barrier disruption in Alzheimer's disease. Brain Pathol 2013;23:303–10
23. Verbeek MM, de Waal RM, Schipper JJ, et al. Rapid degeneration of cultured human brain pericytes by amyloid beta protein. J Neurochem 1997;68:1135–41
24. Wilhelmus MM, Otte-Holler I, van Triel JJ, et al. Lipoprotein receptor–related protein-1 mediates amyloid-beta–mediated cell death of cerebrovascular cells. Am J Pathol 2007;171:1989–99
25. Ozerdem U, Grako KA, Dahlin-Huppe K, et al. NG2 proteoglycan is expressed exclusively by mural cells during vascular morphogenesis. Dev Dyn 2001;222:218–27
26. Stallcup WB, Huang FJ. A role for the NG2 proteoglycan in glioma progression. Cell Adhes Migr 2008;2:192–201
27. Ozerdem U, Stallcup WB. Pathological angiogenesis is reduced by targeting pericytes via the NG2 proteoglycan. Angiogenesis 2004;7:269–76
28. You WK, Yotsumoto F, Sakimura K, et al. NG2 proteoglycan promotes tumor vascularization via integrin-dependent effects on pericyte function. Angiogenesis 2013;7:61–76
29. Fukushi J, Makagiansar IT, Stallcup WB. NG2 proteoglycan promotes endothelial cell motility and angiogenesis via engagement of galectin-3 and alpha3beta1 integrin. Mol Biol Cell 2004;15:3580–90
30. Nielsen H, Ek D, Avdic U, et al. NG2 cells, a new trail for Alzheimer's disease mechanisms? Acta Neuropathol Commun 2013;1:7
31. Nielsen HM, Hall S, Surova Y, et al. Low levels of soluble NG2 in cerebrospinal fluid from patients with dementia with Lewy bodies. J Alzheimers Dis 2014; 40:343–50
32. Gibb WR, Luthert PJ, Janota I, et al. Cortical Lewy body dementia: Clinical features and classification. J Neurol Neurosurg Psychiatry 1989; 52:185–92
33. Nishiyama A. NG2 cells in the brain: A novel glial cell population. Hum Cell 2001;14:77–82
34. Asher RA, Morgenstern DA, Properzi F, et al. Two separate metalloproteinase activities are responsible for the shedding and processing of the NG2 proteoglycan in vitro. Mol Cell Neurosci 2005; 29:82–96
35. Liu H, Shubayev VI. Matrix metalloproteinase-9 controls proliferation of $NG2^+$ progenitor cells immediately after spinal cord injury. Exp Neurol 2011;231:236–46
36. Larsen PH, Wells JE, Stallcup WB, et al. Matrix metalloproteinase-9 facilitates remyelination in part by processing the inhibitory NG2 proteoglycan. J Neurosci 2003;23:11127–35
37. Dreier R, Wallace S, Fuchs S, et al. Paracrine interactions of chondrocytes and macrophages in cartilage degradation: Articular chondrocytes provide factors that activate macrophage-derived pro-gelatinase B (pro-MMP-9). J Cell Sci 2001;114:3813–22
38. Ogata Y, Itoh Y, Nagase H. Steps involved in activation of the pro-matrix metalloproteinase 9 (progelatinase B)–tissue inhibitor of metalloproteinases-1 complex by 4-aminophenylmercuric acetate and proteinases. J Biol Chem 1995;270:18506–11
39. Steenport M, Khan KM, Du B, et al. Matrix metalloproteinase (MMP)-1 and MMP-3 induce macrophage MMP-9: Evidence for the role of TNF-alpha and cyclooxygenase-2. J Immunol 2009;183:8119–27
40. Bouchard BA, Shatos MA, Tracy PB. Human brain pericytes differentially regulate expression of procoagulant enzyme complexes comprising the extrinsic pathway of blood coagulation. Arterioscler Thromb Vasc Biol 1997;17:1–9
41. Verbeek MM, Otte-Holler I, Wesseling P, et al. Induction of alpha-smooth muscle actin expression in cultured human brain pericytes by transforming growth factor-β1. Am J Pathol 1994;144:372–82
42. Tigges U, Welser-Alves JV, Boroujerdi A, et al. A novel and simple method for culturing pericytes from mouse brain. Microvasc Res 2012;84:74–80
43. Verbeek MM, Otte-Holler I, Wesseling P, et al. Induction of alpha-smooth muscle actin expression in cultured human brain pericytes by transforming growth factor-beta 1. Am J Pathol 1994;144:372–82
44. Korzeniewski C, Callewaert DM. An enzyme-release assay for natural cytotoxicity. J Immunol Methods 1983;64:313–20
45. Ramos-DeSimone N, Hahn-Dantona E, Sipley J, et al. Activation of matrix metalloproteinase-9 (MMP-9) via a converging plasmin/stromelysin-1 cascade enhances tumor cell invasion. J Biol Chem 1999;274:13066–76

46. Horstmann S, Budig L, Gardner H, et al. Matrix metalloproteinases in peripheral blood and cerebrospinal fluid in patients with Alzheimer's disease. Int Psychogeriatr 2010;22:966–72
47. Klein WL. Synaptotoxic amyloid-beta oligomers: A molecular basis for the cause, diagnosis, and treatment of Alzheimer's disease? J Alzheimers Dis 2013;33(Suppl 1):S49–65
48. Stefani M. Structural features and cytotoxicity of amyloid oligomers: Implications in Alzheimer's disease and other diseases with amyloid deposits. Prog Neurobiol 2012;99:226–45
49. Biron KE, Dickstein DL, Gopaul R, et al. Amyloid triggers extensive cerebral angiogenesis causing blood brain barrier permeability and hypervascularity in Alzheimer's disease. PLoS One 2011;6:e23789
50. Ujiie M, Dickstein DL, Carlow DA, et al. Blood-brain barrier permeability precedes senile plaque formation in an Alzheimer disease model. Microcirculation 2003;10:463–70
51. Biron KE, Dickstein DL, Gopaul R, et al. Cessation of neoangiogenesis in Alzheimer's disease follows amyloid-beta immunization. Sci Rep 2013;3:1354
52. Dickstein DL, Biron KE, Ujiie M, et al. Abeta peptide immunization restores blood-brain barrier integrity in Alzheimer disease. FASEB J 2006;20:426–33
53. Pieper C, Pieloch P, Galla HJ. Pericytes support neutrophil transmigration via interleukin-8 across a porcine co-culture model of the blood-brain barrier. Brain Res 2013;1524:1–11
54. Yang Y, Estrada EY, Thompson JF, et al. Matrix metalloproteinase–mediated disruption of tight junction proteins in cerebral vessels is reversed by synthetic matrix metalloproteinase inhibitor in focal ischemia in rat. J Cereb Blood Flow Metab 2007;27:697–709
55. Virgintino D, Errede M, Girolamo F, et al. NG2 modulates tight junction integrity in brain microvessels. Ital J Anat Embryol 2011:116
56. Farrall AJ, Wardlaw JM. Blood-brain barrier: Ageing and microvascular disease—systematic review and meta-analysis. Neurobiol Aging 2009; 30:337–52
57. Wang H, Golob EJ, Su MY. Vascular volume and blood-brain barrier permeability measured by dynamic contrast enhanced MRI in hippocampus and cerebellum of patients with MCI and normal controls. J Magn Res Imaging 2006;24:695–700
58. Baloyannis SJ, Baloyannis IS. The vascular factor in Alzheimer's disease: A study in Golgi technique and electron microscopy. J Neurol Sci 2012;322:117–21
59. Buee L, Hof PR, Bouras C, et al. Pathological alterations of the cerebral microvasculature in Alzheimer's disease and related dementing disorders. Acta Neuropathol (Berl) 1994;87:469–80
60. Cordonnier C. Brain microbleeds. Pract Neurol 2010;10:94–100
61. Stallcup WB. The NG2 proteoglycan: Past insights and future prospects. J Neurocytol 2002;31:423–35
62. Stomrud E, Bjorkqvist M, Janciauskiene S, et al. Alterations of matrix metalloproteinases in the healthy elderly with increased risk of prodromal Alzheimer's disease. Alzheimers Res Ther 2010;2:20
63. Bell RD, Winkler EA, Singh I, et al. Apolipoprotein E controls cerebrovascular integrity via cyclophilin A. Nature 2012;485:512–16

